World Conference on
Timber Engineering
Oslo 2023

# REINFORCEMENT OF TIMBER STRUCTURES VERSUS CLIMATE IMPACT

**Bettina Franke[1], Steffen Franke[2], Marcus Schiere[3]**

**ABSTRACT:** Wood is a hygroscopic material. The moisture content of wood changes due to ambient climate variations. The moisture content changes first on the surface and a moisture gradient develops over the cross section and results in moisture induced stresses (MIS). MIS occur in addition to normal stresses for the load-bearing resistance and can affect mechanical reinforcements. The paper shows results from experimental test series on the load, moisture, and deformation investigation of structural glulam members reinforced with internal mechanical fasteners. Stepwise climate scenarios were applied and considered climates experienced by the structural timber member before or after reinforcement. For the estimation of the swelling and shrinkage behaviour, effective hygro-expansion coefficients have been determined. The coefficients are significantly lower than previously assumed in the standards. This enables engineers to estimate more realistic wood deformations and the impact on reinforcements which is not neglectable and reduces damage in a wide range of applications. The research results promote the use of wood by ensuring quality, performance, and aesthetics in timber constructions.

**KEYWORDS:** Wood, reinforcement, self-tapping screws, moisture induced stress, hygro-expansion coefficients

## 1 INTRODUCTION

The performance of structural timber members can be enhanced by mechanical reinforcements e.g., in the form of bonded in rods, self-drilling fully threaded screws or threaded rods. Reinforcements of connections or timber members become necessary by restricted cross-sectional geometry or if e.g., curved, notched, or members with holes are used, as shown among others in [1], [2], [3], [4], [5], [6].

Wood as a hygroscopic capillary porous material adsorb or release water from the ambient air. Directly on the wood surface, an equilibrium moisture content develops, which depends on the relative humidity and temperature. The moisture transport over the cross-section takes place by diffusion and is very prolonged, [7]. Therefore, a moisture profile is formed over the cross-section which leads to moisture induced stresses (MIS) due to the non-uniform shrinkage and swelling of the wood cross section, [8]. In addition, the internal reinforcements not only improve the performance of timber structures but also change/restrict the free deformation behaviour of the cross-section which also leads to MIS. The two aspects, MIS and internal reinforcement, occur together in the life cycle of timber structures. The research done by Danzer et al. [9] shows that the load-carrying capacity of reinforced members with notches can even be reduced compared to unreinforced ones.

The objective is to provide answers to the load-bearing behaviour of reinforced timber constructions exposed to climate changes. The focus is on systematically defined experimental investigations on glulam beams of practical relevance with different reinforcement ratios. The research work focuses on findings on effective hygro-expansion coefficients for internal reinforced glulam members under drying and wetting climate exposure which can be used to estimate shrinkage and swelling deformations as well as additional stresses within the reinforcements.

## 2 STATE OF THE ART

### 2.1 CLIMATE IMPACT

Structural damage related to moisture was quantified by a study in which existing buildings in southern Germany were assessed. Moisture accounted for half of the observed structural damage: too wet, too dry, or varying moisture conditions [10]. The latter accounted for approximately one sixth of the damage in need of repair [11]. About 90% of the encountered damage was found in glued laminated timber. The damage not related to moisture content concerned wrong assumption of loads or errors in calculation of load-bearing capacities for instance.

Varying climatic stresses occur not only in exterior components but also in interior components in non-air-conditioned structures or through specific user profiles, [13], [14]. The analyses of monitoring data show that in heated not climatized structures (generally service class 1 according to EN 1995-1-1:2004 [15]), relative humidity in winter is lower than in summer. In buildings that are not heated but ventilated (generally service class 2 according to EN 1995-1-1:2004), the relative humidity is low in summer whereas it increases towards autumn/winter.

[1] Bettina Franke, Bern University of Applied Sciences, Switzerland, bettina.franke@bfh.ch
[2] Steffen Franke, Bern University of Applied Sciences, Switzerland, steffen.franke@bfh.ch
[3] Marcus J. Schiere, Wijma Kampen B.V., Kampen, Netherland, mjs@hupkeswijma.com

https://doi.org/10.52202/069179-0037

### 2.2 REINFORCEMENTS IN TIMBER STRUCTURES UNDER CLIMATE EXPOSURE

Reinforcements improve in general the load-bearing behaviour, but the full utilization level cannot be applied. The EN 1995-1-1:2004 [15] does not contain information on this reduced load carrying behaviour. Some national annexes or standards provide information for the calculation of the design value of the tensile force acting on the reinforcement, structural information is given on the distances between each other, from the edge of the notch or opening and on the insertion length for curved or pitched roof beams. Guidance on the calculation of the deformation behaviour or the consideration of additional moisture-induced stresses due to single or varying climate changes is not given in standards. It is known that the hygro-expansion coefficient is not fully effective due to viscoelastic behaviour, but only minor information is given, [16].

Research on mechanical internal reinforcements like bonded in rods, self-drilling fully threaded screws or threaded rod, was mainly done for the static short term load-bearing behaviour in constant climate, e.g. [17], [18]. There are first experiences available for reinforced beams under varying dynamic climate, [9], [6], [19], [20]. Sjödin [20] confirms an indeed reduced load-bearing capacity of steel-timber dowel joints loaded parallel to the grain under initial drying exposure. Wallner [19] only investigated processes during restricted shrinkage. There are no studies on restricted swelling, where tensile stresses in the screw can overlap with tensile stresses from external loads, and under varying climates. Likewise, the increasing influence of end-grain moisture transport was not considered. Trautz [6] measured the deformations of self-tapping screws as connectors and reinforcements on rigid frame corners in exterior climatic to evaluate the creep of the screws and the connections. The results for the specimens with a high degree of utilization also show a decrease of load-bearing capacity after an exterior exposure of 2 years.

The fact that damage can occur even in reinforced curved and pitched roof beams, support areas, notches and holes is well known, [21], [22]. Relaxations of 50% are realistic according to SIA 265/1, [16], [23] and would theoretically double the allowable moisture change. Dietsch [24] also states that a moisture reduction of 1% already cancels out the effect of the reinforcement measure. This was calculated for a curved beam and 50% relaxation.

## 3 MATERIAL AND METHOD

### 3.1 MATERIAL

Glulam produced from softwood is still one of the most important building materials in modern timber construction industry and most research focused on softwood members. Hence, GL24h from Spruce was used for the experimental test program. The glulam members were reinforced with 16 mm SFS WB-T threaded screws/rods.

Widths of glulam beams in modern timber engineering range between 160 mm and 240 mm, [13]. In discussions with practical engineers, the heights of glulam beams range from 600 mm to 2000 mm and rarely over 2000 mm. Therefore, the experimental test series comprises unreinforced and reinforced specimens with a standard beam width of 160 mm and heights of 600 mm and 1000 mm. The element lengths were either 160 mm or 320 mm, in line with work performed by Wallner [19]. The size of the elements and reinforcement ratio were chosen such that the reinforcement would have approximately the same stiffness as the glulam member, or twice the stiffness of the glulam member, cf. equation (6).

### 3.2 CLIMATE SCENARIOS

The ambient climate at structural members depends on the building occupation, their use, the meteorological conditions, local topography or environment, and altitude and varies throughout the year. The annual variations can easily be simplified using a sinus shape model, [14]. For further simplification, three stepwise climate changes A, B, and C were used for the experimental test programme considering sudden climate changes experienced by the wood before or after reinforcing (Figure 1). In each case the elements of the test programme were climatized in climate chambers. The start of the three step-climate changes is always related to the moisture content of 12 M% from the production phase.

- In climate scenario A, the climate change represents the reinforcement of the timber member during production directly going into service as in sports hall with a drying/desorption process.
- The climate scenario B also represents a reinforcement of the timber member during production but going into a construction period of 38 days with wetting/adsorption

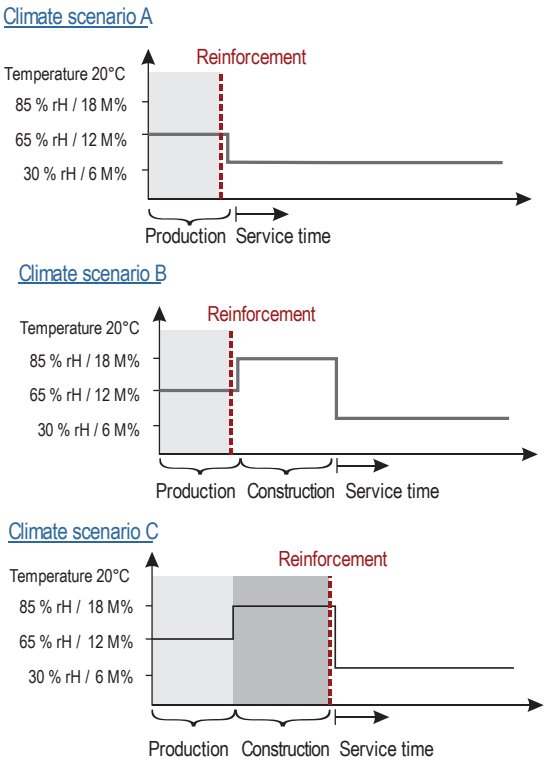


***Figure 1:*** *Illustration of the three stepwise climate scenarios applied within the experimental test programme.*


https://doi.org/10.52202/069179-0037

process before starting service time with a drying/desorption process.

- In climate scenario C, the reinforcement is installed on-site at the end of the construction period of 38 days followed by service with a drying process. This results in a higher moisture load after reinforcing.

### 3.3 EXPERIMENTAL PROGRAMME AND CLIMATE CONDITIONING

The total of 28 test specimens was divided into the three defined climate scenarios A, B, C. Figure 2 shows an overview of the samples used, geometries, reinforcements, and climate loads. The end grains of most of the glulam beams were sealed to represent a continuous beam, only few end-grains were not sealed to represent reinforcements being located close to end grains, as at notches, holes or supports. The end grain sealing was done with aluminium tape.

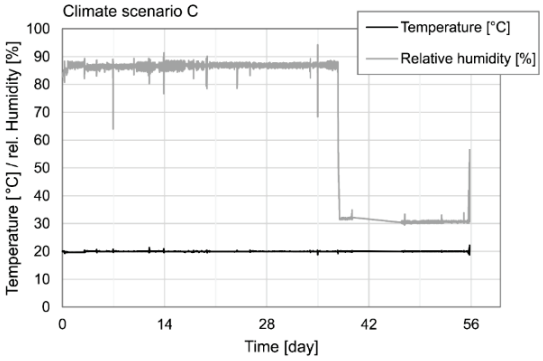


***Figure 3:*** *Recorded climate data for climate scenario C, starting with 85% relative humidity and 20 °C to achieve a moisture content of 18 M%, followed with 30% relative humidity and 20 °C to achieve a moisture content of 6 M%*

To reach the moisture content steps of about 12, 18, and 6 M%, climates of 65, 85, and 30% relative humidity have been used respectively. The temperature was constant at 20 °C. Figure 3 shows representative the climate data for the drying process of climate scenario C. The measurement of climate was performed with calibrated Elprolog TH1 sensors and logged every 10 minutes.

## 4 MEASURING METHODS

### 4.1 MOISTURE CONTENT VARIATIONS/DISTRIBUTIONS

Moisture content variations within the glulam beams were measured using the electrical resistance method. Pairs of partially insulated GANN electrodes of 15 mm, 25 mm, and 40 mm lengths were inserted in predrilled holes at the corresponding measuring depths. The measurements of the electrical resistance were done and logged with the equipment of Scanntronik Mugrauer GmbH. Temperature sensors were installed too for temperature compensation within the conversion process from electrical resistance to the moisture content, [25]. The accuracy of this method lies between 1 M% to 2 M%, [25]. The moisture content at the surface was taken as equilibrium moisture content calculated from the surrounding climate using the Simpson equation, [26]. The measurement frequency was 1 hour.

Each measurement point was named according to the element number, the type of measurement, the location, and the length of the electrode:

- Px, specimen name/number
- HF, moisture content
- MI for middle (lengthwise) and SH for end grain
- 15, 25 or 40, measuring depth/length of electrode pair in millimetres

The name P3-HF-MI-15 represents the moisture content measurement, midsection at 15 mm depth of the test specimen P3.

| Climate scenario | 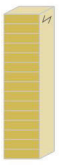 unreinforced unsealed | 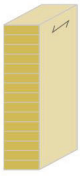 unreinforced unsealed |   unreinforced sealed |   reinforced unsealed | 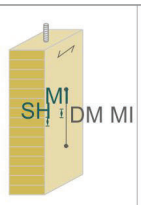  reinforced unsealed | 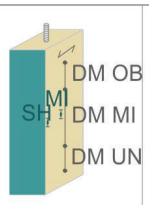  reinforced sealed | 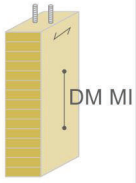  reinforced unsealed |
|---|---|---|---|---|---|---|---|
| [mm] | 160/160/600 | 160/320/600 | 160/320/600 | 160/160/600 | 160/320/600 | 160/320/600 | 160/320/600 |
| A | # P9 | # P10 | # P23 | # P1 | # P2[1)] | # P3[1)], P11[1)], P12 | # P4 |
| B | | | # P25 | - | - | # P15[2)], P16 | - |
| C | | | # P27 | # P5 | # P6[1)] | # P7[1)], P19[1)], P20 | # P8 |

[1)] Measurment of moisture content in depths of 15 and 40 mm
[2)] Measurment of moisture content in depths of 15, 25, and 40 mm

***Figure 2:*** *Overview of all experimental test series considering the climate scenarios and individual configuration*

https://doi.org/10.52202/069179-0037

### 4.2 DEFORMATION OF THE REINFORCEMENT

For the estimation of the deformation behaviour of the reinforcement, a measuring frame with gauge was used. The deformations of the reinforcement within a 600 mm high beam were estimated to be around 2 mm ($E_{t,90,m}$ = 300 N/mm$^2$ and $\alpha_{90}$ = 0.25%/M%) when reaching the tension strength perpendicular to the grain of $f_{t,90}$ = 0.5 N/mm$^2$ (EN 14080:2013). Therefore, a measuring frame/rig was constructed and equipped with a dial gauge of 10 mm measuring range and 0.01 mm measuring resolution, Figure 4. To reduce measurement uncertainties due to thermal expansion, a reference bar from the same material was measured together with the glulam beams and elongations were corrected. The errors lie within the measurement resolution of the gauge but remain small (order of 1/100th of a millimetre). Right after the start or the change of the climate, the deformations were measured more often than close to the end of the tests.

### 4.3 DEFORMATION OF THE GLULAM BEAM

For the deformation of the timber elements at the surface, a deformeter with measuring range of 100 mm and 200 mm was used. Before each measurement, the deformeter was calibrated using fixed reference bars.

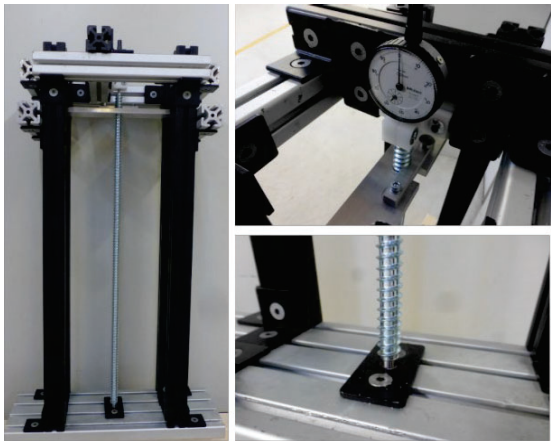

***Figure 4:*** *Picture of the constructed frame (left) to measure 600 mm high beam with a gauge at the top (top right) and a nut (bottom right) to fit the screw into on the bottom*

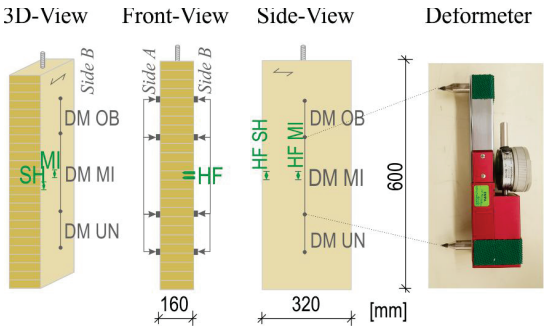


***Figure 5:*** *Illustration of the positions and naming of the measurement of deformations on the wood surface of glulam beams as 3D-, front- and side view using the deformeter (right)*

Measurements were made on both sides of the beams and averaged, see Figure 5. Because an eccentricity in loading of 10% (width $b$ and height $h$) lead to a measurement error of 60% if strains are measured on one side only. Averaging these two strains results in a representative strain.

$$\varepsilon_{\pm h/2} = \frac{F}{AE} \pm \frac{My}{IE} = \frac{F}{AE} \pm \frac{0.1hF0.5h}{IE}$$
$$\varepsilon_{\pm h/2} = \frac{F}{E}\left(\frac{1}{bh} \pm \frac{12h^2}{20h^3b}\right) = \frac{F}{Ebh}(1 \pm 0.6) \quad (1)$$

## 5 EXPERIMENTAL RESULTS

### 5.1 MOISTURE CONTENT MEASUREMENTS

The moisture content measurements are plotted in Figure 8. Since not all specimens could be equipped with moisture measurement sensors, the measured values are applied to all specimens of the same climate/group for further analyses.

The intended pre-climatization of the elements to a moisture content of 12 M% and 18 M% was not fully achieved for climate scenario A and C respectively.

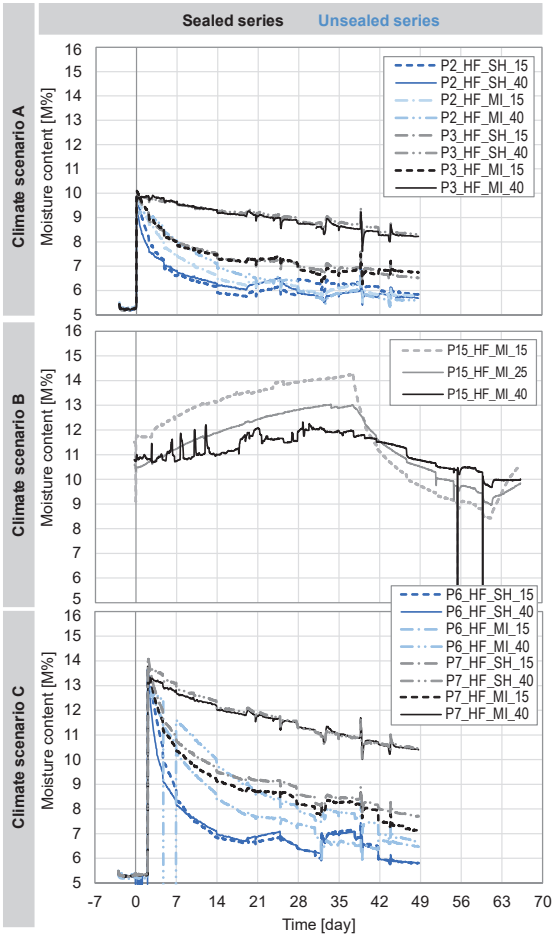


***Figure 6:*** *Moisture content development of the three different climate scenarios, shown for the test specimen per series over the different depths observed*


https://doi.org/10.52202/069179-0037

Instead, moisture content levels of 10 M% and 14 M% were achieved because of too low relative humidity set up and conditioning time estimated. The climatization of the second series (P11 to P27) was adapted accordingly. To achieve the moisture content of 18 M%, the elements were stored in a climate chamber with a relative humidity of 85%. Instead of maintaining the temperature at 20 °C, like was done in the first series, a higher temperature of nearly 40 °C was maintained. In addition, the elements were artificially wetted by spraying water onto the end grains of the elements to accelerate the climatization. In the second series, the achieved moisture content at the start of the tests was around 13 M% and 18 M%.

The function of sealing can clearly be seen; the moisture transport in general is reduced. Once the end grain is not sealed like in P2 and P6, the moisture content on the cross section reduces more rapidly and equilibrium is reached after about 20 days. There is not only a moisture gradient along the width of the element but also along the length of the element. Whereas equilibrium is not reached for the sealed ones within 50 days (P3 and P7) and there is almost no difference between the measuring points in the centre (MI) and near the end grain surface (SH).

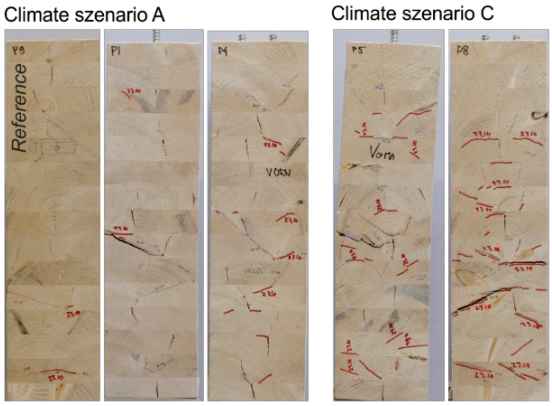


***Figure 7:*** *Cracking pattern of the end grains for reference specimen P9 and specimens with double reinforcement stiffness P1, P4, P5, and P8 (l.t.r.)*

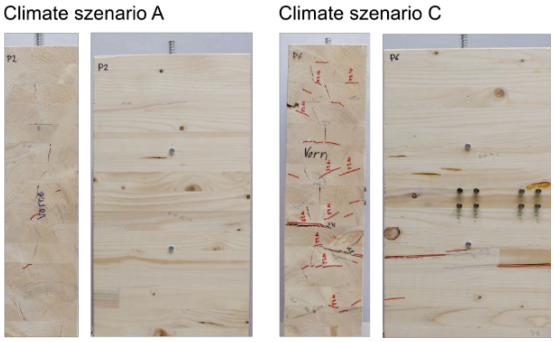


***Figure 8:*** *Cracking pattern of the end grains for reference specimen P9 and specimens with double reinforcement stiffness P1, P4, P5, and P8 (l.t.r.)*

### 5.2 CRACK GROWTH BEHAVIOUR

Cracking was recorded for all specimens as e.g., shown in Figure 7 and Figure 8. For the higher moisture load of about $\Delta = 12$ M% (climate scenario C) more cracks developed at the end grain and even cracks on the side are visible. Almost no cracks are visible at the side for the lower moisture load with $\Delta = 6$ M% (climate scenario A). Specimen with single reinforcement show pronounced larger cracks on one side together with quite large bending deformations compared to the specimen with double reinforcements.

The relation between moisture content change and crack growth is illustrated in Figure 9. The cracked specimens show in average slightly smaller moisture content changes at time of failure compared to the uncracked specimens. P19 was perhaps prone to cracking, as a crack was visible already before the test starts.

### 5.3 DEFORMATION AND STRAIN

The measured deformations at the reinforcement and at the timber surface are shown as strains for each climate scenario and configuration in Figure 10. It can be seen that:

- Small moisture content changes (elements P1 to P4) have high deformation; medium moisture content changes (P5 to P8 and P11 to P14) lead to small deformation.
- An effect of the double reinforcement on 600 mm high elements is observed (P4/P2 ≈ 0.8 and P8/P6 ≈ 0.5)

## 6 EVALUATION OF THE EFFECTIVE HYGRO-EXPANSION COEFFICIENT

Based on the measured change of moisture content, the dependency of the strain of the reinforcement on moisture content change can be calculated too. This is like a hygro-expansion coefficient with the unit as %/M%. The effective hygro-expansion coefficient is calculated by Equation (5). This is based on a model for composite structures consisting of two different materials 1 and 2 with assuming equal strain in the materials, as shown in Figure 11 and expressed by following equations (2) to (6):

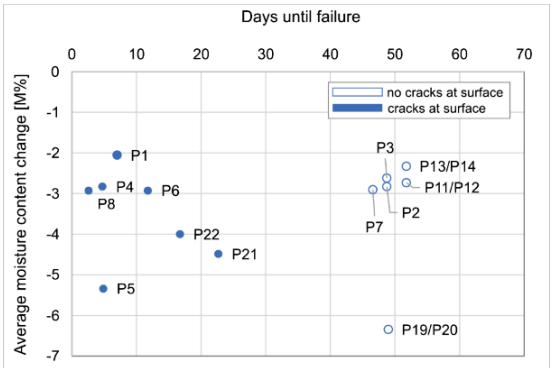


***Figure 9:*** *Relation between days until failure and changed moisture content at time of failure*

https://doi.org/10.52202/069179-0037

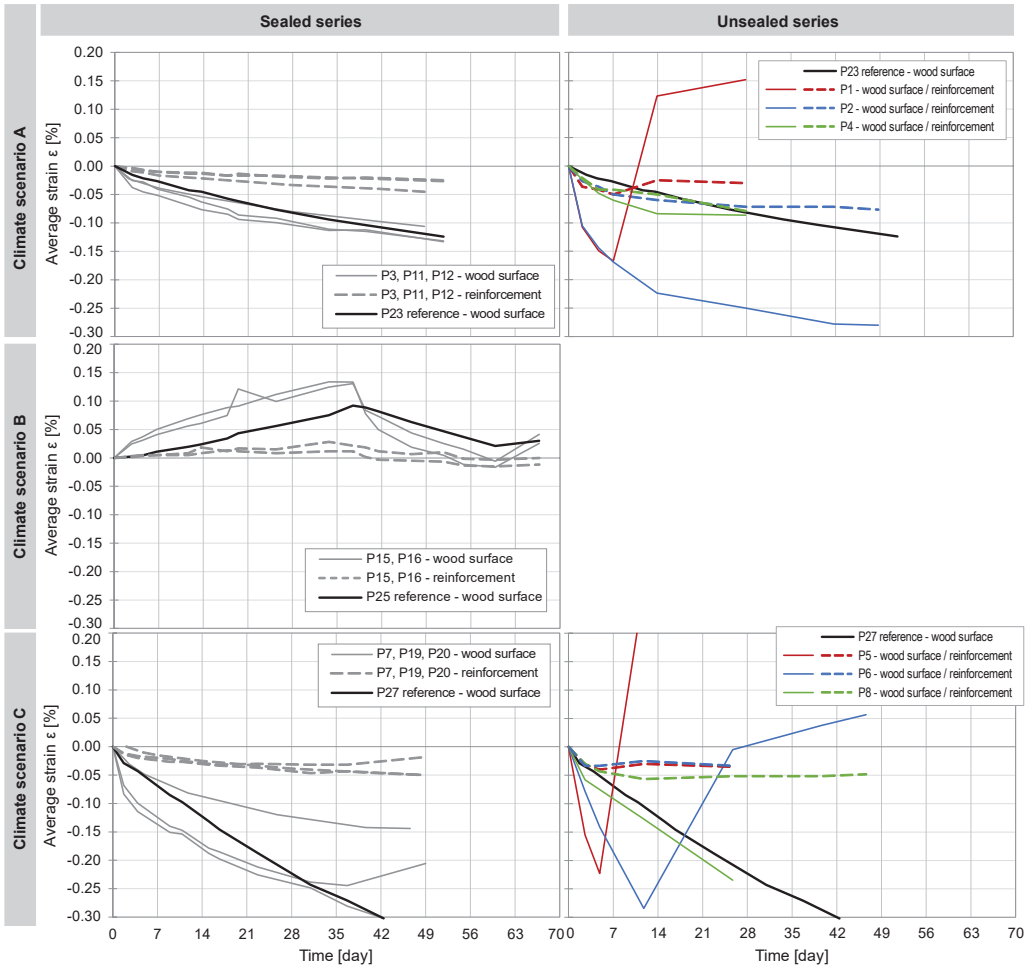


***Figure 10:*** *Strain development in the reinforcement and on the surface separated for the sealed and unsealed specimens*

$$\Delta\varepsilon = \Delta\sigma / E + \alpha\Delta u \tag{2}$$

$$\Delta\varepsilon_0 = \left(F_e + \alpha_1 \Delta u_1 A_1 E_1\right) / \left(A_1 E_1 + A_2 E_2\right) \tag{3}$$

$$\begin{aligned} \Delta\sigma_1 &= \left(\left(F_e + \alpha_1 \Delta u_1 A_1 E_1\right) / \left(A_1 E_1 + A_2 E_2\right) - \alpha_1 \Delta u_1\right) E_1 \\ \Delta\sigma_2 &= \left(F_e + \alpha_1 \Delta u_1 A_1 E_1\right) / \left(A_1 E_1 + A_2 E_2\right) E_2 \end{aligned} \tag{4}$$

$$\begin{aligned} \Delta\sigma_1 &= \alpha_1 \Delta u_1 \left(\gamma - 1\right) E_1 \\ \Delta\sigma_2 &= \alpha_1 \Delta u_1 \gamma E_2 \end{aligned} \tag{5}$$

with $\gamma$ as the ratio of stiffness between the timber cross section and the total cross-section, a value between 0 and 1:

$$\gamma = \frac{A_1 E_1}{A_1 E_1 + A_2 E_2} \tag{6}$$

The stress in the reinforcement is calculated from the strain corrected with the S-factor of 1.42 for 600 mm high beams considering the non-uniform strain distribution over the depth of the beam, cp. Figure 11. Furthermore, a correction on height of the specimen is also done to obtain the stresses in an infinitely high specimen. Therefore, investigation with different depths can directly be compared. The stresses in the reinforcement from the 600 mm high specimens are therefore corrected by a coefficient of 0.68. All strains and wood moisture content are taken from the last measurement before fracture was observed or at the end of the climatization.

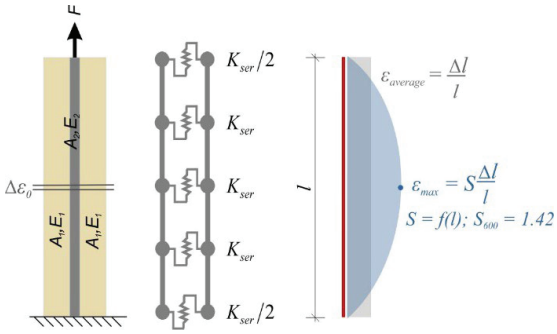


***Figure 11:*** *A composite structure consisting of two different materials 1 and 2*


https://doi.org/10.52202/069179-0037

Figure 12 shows the calculated values as a function of time for the test specimens of climate scenario A. The hygro-expansion coefficient ends up between 0.05 and 0.10%/M% for this specimen series. Only specimen P1 shows much higher values just at the beginning of the climate change. This was also the time when fracture occurred.

The calculated effective hygro-expansion coefficients before failure are plotted in relation of the final moisture content changes the elements experienced just before the failure, see Figure 13. The value from specimen P1 can be excluded due to the early failure and the unsafe value. In average, an effective hygro-expansion coefficient of 0.055%/M% are calculated. No difference in the hygro-expansion coefficient between elements with or without end grain sealing or drying and wetting processes are observed. Generally, the expansion of the reinforcement is therefore about 1/5$^{th}$ of the hygro-expansion coefficient of wood perpendicular to the grain (0.24 %/M%, SIA 265).

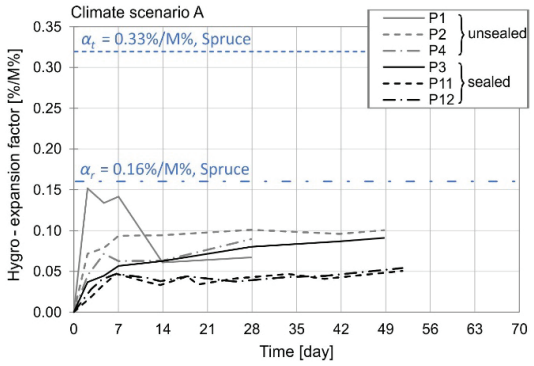


***Figure 12:*** *Calculated hygro-expansion coefficients development for climate scenario A over time*

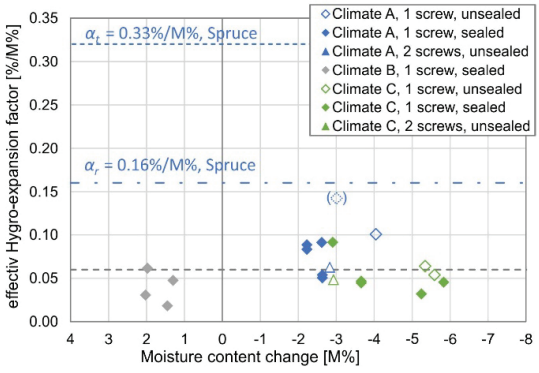


***Figure 13:*** *Derivation of the effective hygro-expansion coefficient of the glulam cross-section according to the composite structure theory*

## 7 CONCLUSIONS

The calculated effective hygro-expansion coefficients for all specimens and climate scenarios presented show a quite constant reduced coefficient compared to the hygro-expansion coefficients for free swelling and shrinkage or even the half value for restricted shrinkage as specified in [16].

Using a simplified model, effective hygro-expansion coefficients could be calculated. In these calculations, theoretical design values for E-moduli (300 N/mm $^2$) had to be used. An important conclusion is that whereas theoretical hygro-expansion values of wood perpendicular to the grain lie around 0.24%/M% (SIA 265, 2012), these might lie close to a fifth of this value in reality. This explains why larger moisture content values are possible without cracking and reflect reality more. To what extend this value is valid for other cross section ratios need to be proved.

Using a value of 0.055%/M% in combination with a correction for a height effect, allows estimation of realistic moisture induced strain changes of reinforced glulam cross-sections. The 0.055%/M% does not reflect the real hygro-expansion coefficient but is expected to be more of an 'effective' value that includes effects of mechano-sorptive relaxation and time-dependent creep too under the presence of reinforcements. To calculate the possible generated additional stress in a cross section due to moisture content changes, Equations (5) can be used where a hygro-expansion coefficient of 0.05%/M% is recommended.

## ACKNOWLEDGEMENT

The research work was funded by Swiss Federal Office of Environmental under the Grant WHFF 2018.14. Thank you too to the research partners, experts and companies who supported the work.

## REFERENCES

[1] H.J. Blass, I. Bejtka, T. Uibel. Tragfähigkeit von Verbindungen mit selbstbohrenden Holzschrauben mit Vollgewinde, *Universitätsverlag Karlsruhe*, 2006.

[2] H.J. Blass, O. Krüger Schubverstärkung von Holz mit Holzschrauben und Gewindestangen, *Karlsruher Berichte zum Ingenieurholzbau*, Band 15, 2010.

[3] H.J. Blass. Selbstbohrende Schrauben und Systemverbinder - Stand der Technik und Herausforderungen, *23. Internationales Holzbau-Forum*, Garmisch-Partenkirchen, 2017.

[4] P. Dietsch. Einsatz und Berechnung von Schubverstärkungen für Brettschichtholzbauteile. *Phd-Thesis*. Technical University Munich, 2012.

[5] P. Dietsch. Effect of reinforcement on shrinkage stresses in timber members. *Construction and Building Materials*, 150, 903-915, 2017.

[6] M. Trautz, C. Koj. Mit Schrauben fügen und bewehren - Langzeitversuche an biegesteifen Rahmenecken im Außenklima, *Bautechnik* 91 (1), 38-45, 2008.

[7] H. Kopfer. Wassertransport durch Diffusion in Feststoffen. *Bauverlag GmbH*, Wiesbaden, Germany, 1974.
[8] Jönsson, J. and Svensson, S. (2004) A contact free measurement method to measure internal stress states in glulam. Holzforschung, 58, 148–153.
[9] M. Danzer, P. Dietsch, S. Winter. Effect of shrinkage on cracking and structural behaviour of reinforced glulam members, *Construction and Building Materials*, 327, 1-14, 2022.
[10] M. Frese, H.J. Blass Statistics of damages to timber structures in Germany, Engineering Structures, 33 (11), 2969–2977. 2011
[11] Dietsch, P., Winter, S., 2018. Structural failure in large-span timber structures: A comprehensive analysis of 230 cases. Journal of Structural Safety, 71, 41-46.
[12] P. Dietsch. Reinforcement of timber structures – A new section for Eurocode 5, World Conference on Timber Engineering, Vienna, 2016.
[13] A. Gamper, P. Dietsch, M. Merk. Gebäudeklima - Langzeitmessung zur Bestimmung der Auswirkungen auf Feuchtegradienten in Holzbauteilen. *Research Report*, TU Munich, Germany, 2012.
[14] B. Franke, S. Franke, M. Schiere, A. Müller. Quality assurance of timber structures. *Research report*, Bern University of Applied Sciences, Switzerland, 2019.
[15] EN 1995-1-1, Eurocode 5. Design of Timber Structures – Part 1-1: General – Common Rules and Rules for Buildings, European Committee for Standardization, Brussels, Belgium, 2004
[16] H.J. Blaß, J. Ehlbeck, H. Kreuzinger, G. Steck. *Erläuterungen zu DIN 1052:2004-08 Entwurf, Berechnung und Bemessung von Holzbauwerken*, DGfH Innovations und Service GmbH München, 2004.
[17] H. Danielsson. *Perpendicular to grain fracture analysis of wooded structural elements - models and applications.* PhD Thesis, Lund University, Sweden, 2013.
[18] R. Jockwer. *Structural behaviour of glued laminated timber beams with unreinforced and reinforced notches.* Ph Thesis. ETH-Zurich, 2014.
[19] B. Wallner. *Versuchstechnische Evaluierung feuchteinduzierter Kräfte in Brettschichtholz verursacht durch das Einbringen von Schraubstangen*. Msc Thesis. TU Graz, 2012.
[20] Sjödin, J. (2008) *Strength and moisture aspects of steel-timber dowel joints in glulam structures - an experimental and numerical study*, Thesis (PhD). Växjö University.
[21] P. Dietsch, R. Brandner. Reinforcement with self-tapping screws and threaded rods in Reinforcement of timber structures: a state-of-the-art report. *Construction and Building Materials*, 97, 78–89, 2015.
[22] Franke, S., Franke, B., Harte, A.M., 2015. Failure Modes and reinforcement techniques for timber beams – State of the Art, Construction and Building Materials, 97, 2-13.
[23] S. Aicher, G. Dill-Langer. Climate induced stresses perpendicular to the grain in glulam, *Otto-Graf Journal,* 8, 209-231, 1997.
[24] P. Dietsch. Effect of reinforcement on shrinkage stresses in timber members, *Construction and Building Materials 150*, pp. 903-915, 2017.
[25] Forsén, H., Tarvainen, V., 2000. Accuracy and functionality of hand-held wood moisture content meters, VTT Publications 420, Technical Research Centre of Finland, Finland.
[26] Simpson W. (1973), Predicting equilibrium moisture content of wood by mathematical models, Wood and Fiber, 5 (1), p. 41-49
[27] M. Danzer, P. Dietsch, S. Winter. Shrinkage behavior of reinforced glulam members, *INTER Conference proceedings*, Karlsruhe, 2020.
[28] SIA 265:2012, Holzbau. Schweizerischer Ingenieur- und Architektenverein, Zürich


https://doi.org/10.52202/069179-0037